Justification of the Modeling Assumptions in the Intermediate Fidelity Models for Portable Power Generation

Internal Report

Alexander Mitsos, Benoît Chachuat and Paul I. Barton*

Department of Chemical Engineering

Massachusetts Institute of Technology,

66-464, 77 Massachusetts Avenue

Cambridge, MA 02139

mitsos@mit.edu, bchachua@mit.edu, pib@mit.edu

tel: 617-253-6526, fax: 617-258-5042

February 8, 2005

1 Abstract

The purpose of this report is to provide a justification for the following modeling assumptions

- Spatially uniform temperature
- Neglecting radial effects in the mass and species balances (1-d)
- Convective flow (neglecting axial diffusion for mass and species-balance)
- Pseudo-steady-state species balances

used in our intermediate fidelity models in [5, 4, 3]. We largely follow the notation in [6], as well as some of the scaling techniques presented there. We assume that we can look sequentially at the assumptions; we first consider the assumption regarding the uniform temperature for a transient problem without gas flow and steady-state problems with gas flow; we then discuss the mass and species balances used, assuming a uniform temperature.

2 Uniform Temperature in the Stack

Our models assume a stack with a uniform temperature (reactor, fuel cell and burner share the same temperature). This was motivated by the fact that heat transfer at this scale is quite fast and the micro-fabricated devices of interest are based on silicon, which is a relatively good heat conductor. Another motivation were our simulations of the reactors of Arana and Jensen [2, 1] and photographs by the same authors suggesting an approximately uniform temperature for reactors with catalyst support under proper operation. For the models considered this approximation is valid for all units; note that a lumped model is used for the fluidic connections. For drastically different approaches, e.g., homogeneous combustion [7, 8] this assumption may not be appropriate, or only valid in subregions.

2.1 Steady-State Case

2.1.1 Scaling Analysis

Because thermal conductivity in silicon is much higher than in the gas phase, catalyst support structures (posts, slabs, etc.) result in significantly increased heat transfer. As an approximation to describe this increase we are using volume-averaged values; assuming a volume ratio of gas/solid 1:1 and a good conductor for the catalyst support, the average heat conductivity is approximately half of the solid. Also the small length between catalyst support in the radial direction allows approximate thermal equilibrium between the gas and solid (locally).

Convection versus conduction

The ratio of convection and conduction is given by

$$\frac{k_{av}}{c_{p,g}\,\rho_g\,u\,L} \approx \frac{10\mathrm{W/m/K}}{10^3\mathrm{J/kg/K} \times 0.5\mathrm{kg/m^3} \times 1\mathrm{m/s} \times 10^{-3}\mathrm{m}} \approx 10,$$

where we have used conservative estimates; conduction (in the silicon-structures) is therefore much more important than convection (through the gas phase).

Estimation of maximal temperature difference

The maximal temperature within a reactor is essentially determined by the ratio of heat transfer within the reactor and heat losses to the ambient. Because of the high temperatures, heat losses to the ambient are dominated by radiation and the heat transfer per unit area can be approximated as $\epsilon\,\sigma_{SB}\,T_{if}^4$, where ϵ is the product of emissivity and view factor, $\sigma_{SB} = 5.67 \times 10^{-8}\mathrm{W/m^2/K^4}$ the Stefan-Boltzmann constant and T_{if} the temperature at the interface. Heat transfer inside the reactor is characterized by the (average) heat conductivity k_{av} divided by the characteristic length L. Therefore the maximal temperature difference can be estimated as

$$\Delta T = \frac{\epsilon\,\sigma_{SB}\,T_{if}^4 L}{k_{av}} \approx \frac{0.1 \times 5.67 \times 10^{-8}\mathrm{W/m^2/K^4} \times 1300^4\mathrm{K}^4 \times 5 \times 10^{-3}\mathrm{m}}{10\mathrm{W/m/K}} \approx 10\mathrm{K},$$

where we have used conservative estimates. This justifies the assumption of uniform temperature.

2.1.2 3d-CFD Duct-Reactor Simulation

Here we examine the effect of averaging the heat conductivity and the assumption of uniform temperature using a duct-reactor, of width and height 500μm and length 2.5mm, pictured in Figure 1.[1]. Our model also includes a 1mm long inlet and outlet to the reactor; we assume that the reactor contains 4 Si-slabs as catalyst support which cover $\frac{2}{5}$ of the width. We assume an inlet velocity of 1m/s. For the simulations we used the finite element package Femlab, and Navier-Stokes equations with variable density and conduction-convection equations for the energy balance. The chemistry was not modeled, but rather a heat generation term was used.[2] Heat losses to the ambient were considered as boundary conditions.

Figure 1 shows that using volume-averaged heat conductivity instead of explicitly modeling the slabs qualitatively and quantitatively captures the effect of increased heat transfer of the catalyst support structure; also the temperature within the reactor portion is essentially uniform. Modeling the slabs explicitly increases the modeling and computational requirements significantly and makes convergence much more demanding.

For the volume-averaged model we explore three cases for the heat generation, namely constant, linear

[1] Exploring the symmetry we only model a quarter of the geometry

[2] When the slabs are modeled explicitly this is introduced as a surface term; for the volume averaged model a volume heat generation is used.

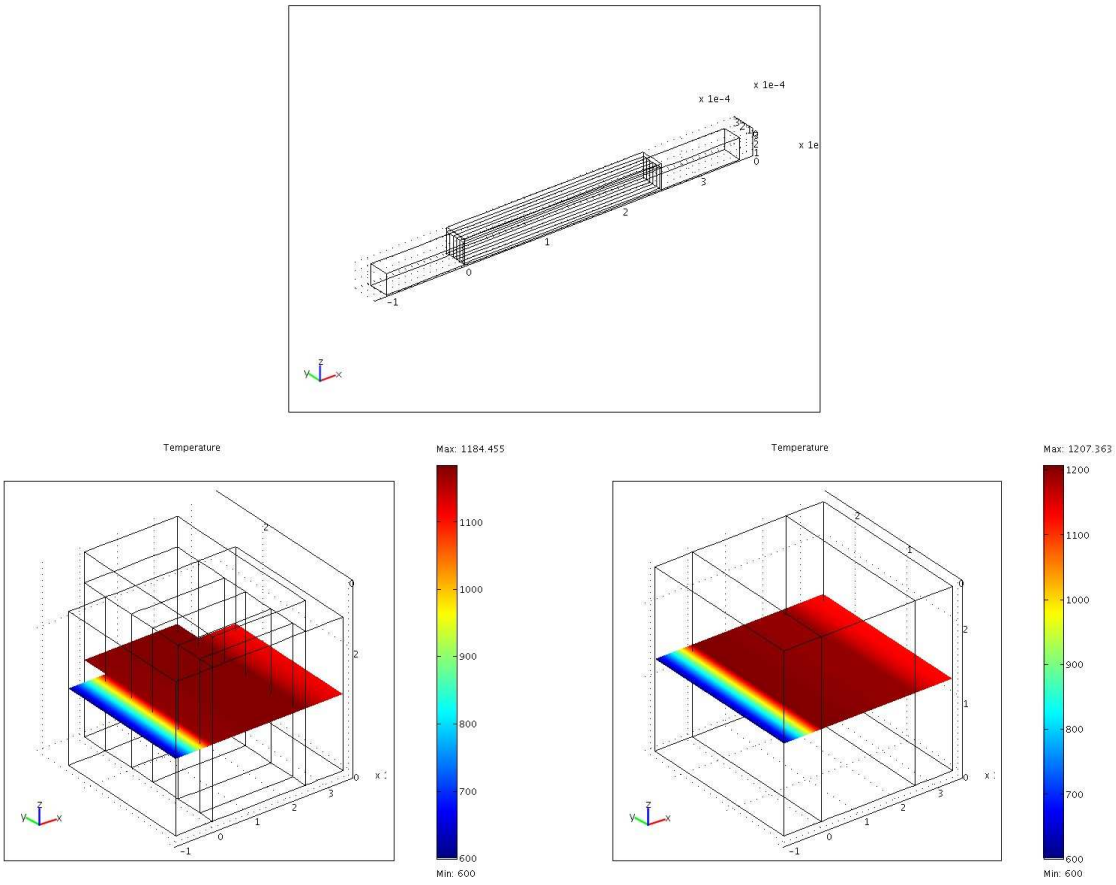

Figure 1: Geometry and temperature profiles for explicit modeling of catalyst support (left) and lumped model (right). Note that for the temperature profiles, a stretching of the axis is performed.

and exponential dependence on the axial coordinate[3]. In Figure 2 the temperature is plotted along the axial coordinate for these three cases as well as the case with explicit modeling of the slabs. The temperature in the reactor portion is essentially uniform, while in the inlet and outlet (where no Si-structure is present) there is a temperature gradient; also the differences between the different heat generation terms are relative small.

[3]The integral of the heat generation is the same in all cases

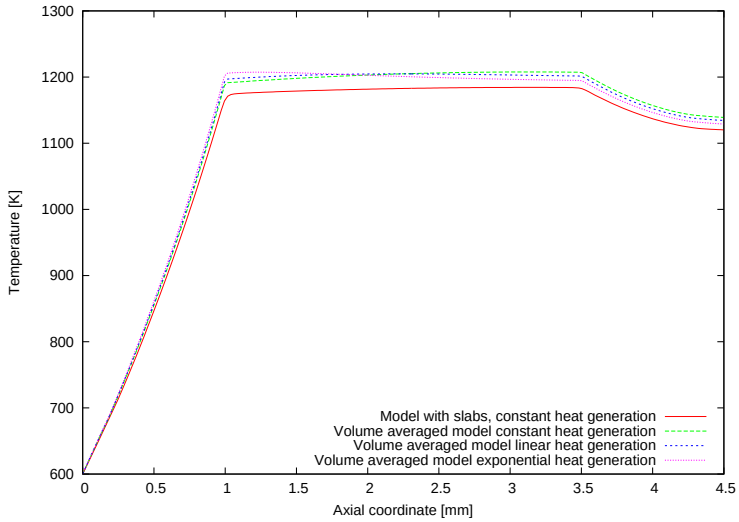

Figure 2: Temperature profiles for explicit and average modeling of slabs.

2.1.3 2d-CFD Reactor Simulation with volume-averaged heat conductivity

Here we briefly discuss the results of computational fluid dynamic analysis of a reactor by Arana and Jensen.[4] The reactor geometry along with the obtained temperature profiles are shown in Figure 3; it should be noted that the reactor design while similar to the ones described in [2, 1] has a different gas flow pattern; here the two portions of the reactor (for endothermic and exothermic reaction respectively) are cocentric, as opposed to parallel as in the design described in the references. For the simulations we used the finite element package Femlab, and Navier-Stokes equation with variable density and conduction-convection for the energy balance. The chemistry was not modeled, but rather a heat generation and heat consumption term was introduced, based on complete conversion. Also the catalyst support was not modeled, but rather a volume-averaged heat conductivity was used. One sees in Figure 3 that without catalyst support ($k = k_g$) there is a significant temperature gradient, while with catalyst support ($k = k_{av}$) the temperature difference within the reactor is relatively small. Note that the temperature profiles are plotted in a stretched geometry.

[4]The modeling details, e.g., boundary conditions, solvers used, convergence scheme, discretization are out of the scope of this report.

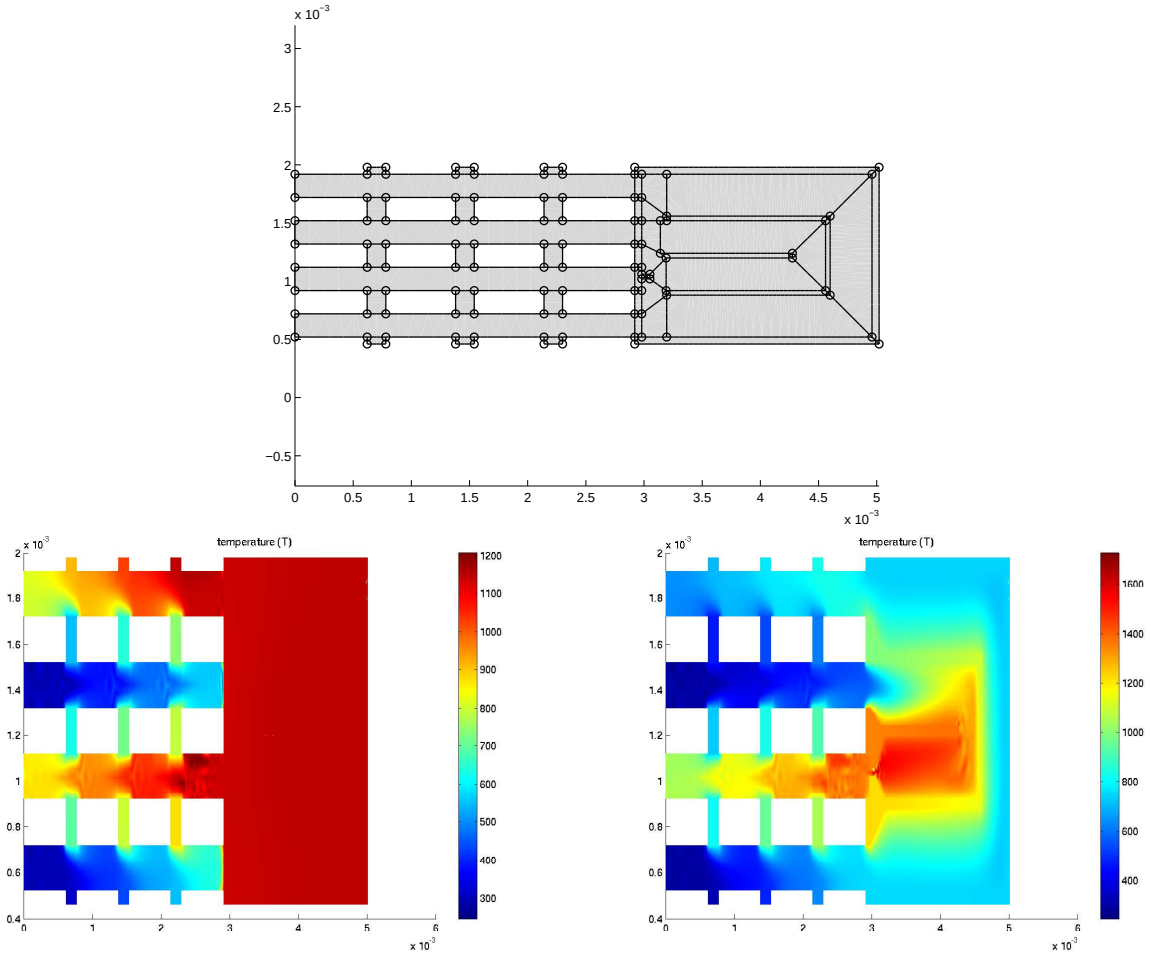

Figure 3: Reactor geometry and temperature profiles obtained by CFD simulation corresponding to reactor with and without catalyst support

2.2 Transient Case

In this subsection we examine the assumption of uniform temperature in the transient case. We consider two geometries:

1. A cubic stack of length L with all but one sides/faces adiabatic and we apply a heat load $\dot{Q}$ on the other side/face, Figure 4. For this geometry we develop a two-dimensional and a three-dimensional model in FEMLAB.

2. A cubic stack of length L, in which a small heating element is placed in the middle, Figure 5. For this geometry we develop a three-dimensional model in FEMLAB.

It should be noted that the considered geometries are extreme cases; for good reactor designs the heat generation (and consumption) should be distributed in space and the resulting characteristic length for heat conduction is much smaller than the reactor dimensions. The magnitude of the heat load is chosen to heat the stack within a time τ from T_i to T_f; its numerical value is approximately 1W. We ignore flow through the system and take average physical properties. For both geometries we perform an analysis based on [6].

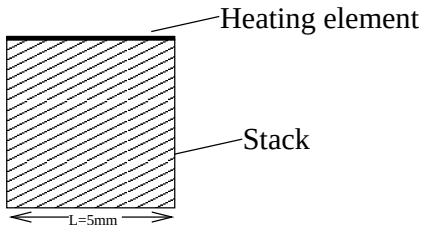

Figure 4: Stack with a heating element in the top

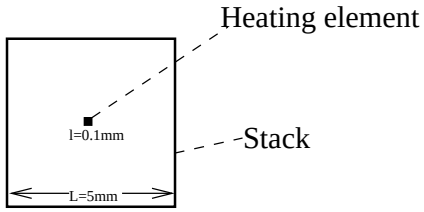

Figure 5: Stack with a heating element in the middle

2.2.1 Scaling Analysis

Neglecting the convective flow and assuming constant physical properties the energy balance reads

$$\rho c_p \frac{\partial T}{\partial t} = k \nabla^2 T \tag{1}$$

We nondimensionalize equation (1) by using the following scaling

- The temperature is nondimensionalized, so that the initial temperature corresponds to a value of 0 and the final temperature to a value of 1: $\tilde{T} = \frac{T - T_i}{T_f - T_i}$.
- The time is nondimensionalized so that the initial time corresponds to a value of 0 and the final time

to a value of 1 $\tilde{t} = \frac{t}{\tau}$.

- The space vector is nondimensionalized by dividing through the characteristic length L: $\tilde{\mathbf{x}} = \frac{\mathbf{x}}{L}$.

We therefore obtain

$$\begin{aligned} \rho c_p \frac{T_f - T_i}{\tau} \frac{\partial \tilde{T}}{\partial \tilde{t}} &= k \frac{T_f - T_i}{L^2} \tilde{\nabla}^2 \tilde{T} \\ \Rightarrow \quad \frac{\partial \tilde{T}}{\partial \tilde{t}} &= \frac{k}{\rho c_p} \frac{\tau}{L^2} \tilde{\nabla}^2 \tilde{T} \\ &= \frac{\alpha \tau}{L^2} \tilde{\nabla}^2 \tilde{T} \end{aligned} \tag{2}$$

When the ratio $\frac{\alpha \tau}{L^2}$ is high, corresponding to a fast heat transport relative to the time scale of change, the temperature in the stack can be considered uniform in space (the term $\tilde{\nabla}^2 \tilde{T}$ needs to be very small, since it is multiplied by a very large number). In the micro-SOFC we have (physical properties for Silicon)

- $\rho \approx 2300 \text{kg/m}^3$
- $c_p \approx \frac{20 \text{J/mol/K}}{0.028 \text{kg/mol}} \approx 700 \text{J/kg/K}$.
- $k \approx 145 - 32 \text{W/m/K}$ in the considered temperature range $T = 300 - 1000 \text{K}$
- $\tau \approx 100 \text{s}$
- $L \approx 1 \text{mm} - 5 \text{mm}$,

so that the ratio $\frac{\alpha \tau}{L^2}$ takes values in the order of $10 - 1000$. For characteristic lengths in the order of cm the ratio can be in the order of 1.

2.2.2 FEMLAB simulation

The transient two- and three- dimensional simulations in FEMLAB validate the previous analysis; the geometries appear of nearly uniform temperature. The parameters used were:

- $L = 5 \text{mm}$

- $k = 70\text{W/m/K}$, corresponding to an average between air and Silicon
- $\rho = 1100\text{kg/m}^3$, corresponding to an average between air and Silicon
- $c_p = 700\text{J/kg/K}$

As boundary conditions we include heat losses to the ambient; a uniform temperature of 300K is taken as the initial condition.

2.2.3 Heating element on top

A movie of the heating is not informative, because, for a temperature range $300 - 1000\text{K}$, the box appears to have completely uniform temperature (uniform color) and we therefore plot the temperature range at given times. In Figure 6 note the plotted temperature interval is approximately 1K.

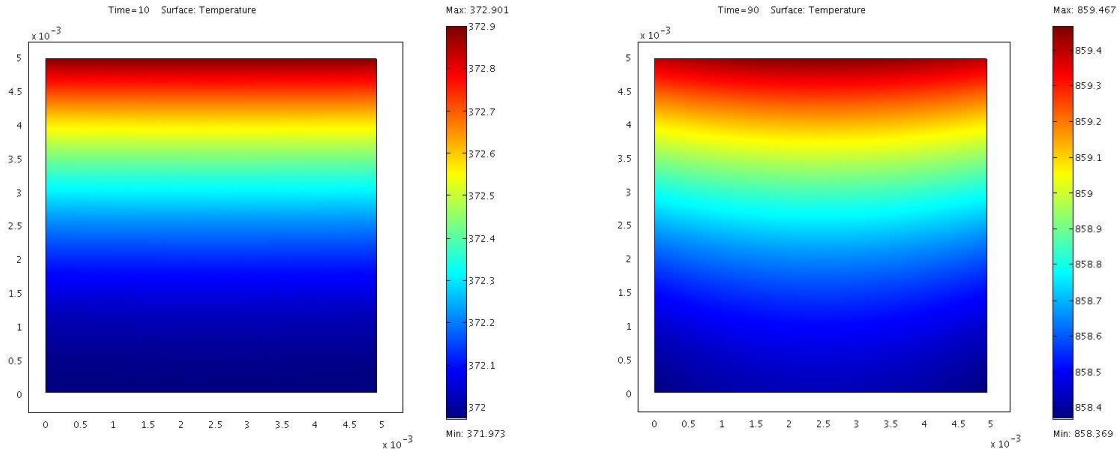

Figure 6: Two dimensional model with heating element on top

2.2.4 Heating element in the middle

Only around the small box there is a small region with temperature gradient; depending on the physical properties used (Si at 1000K, Si at 300K, volumetric average of Si and air) there is a 15-50K difference in this small region. The bulk of the stack has uniform temperature (less than 5K difference). In Figure 7 we plot the temperature for two regions at a simulation time of 70s. Note that the two regions have a different

scale; for the region around the heating box we use a temperature range of 15K, whereas for the outside region an interval of 0.1K.

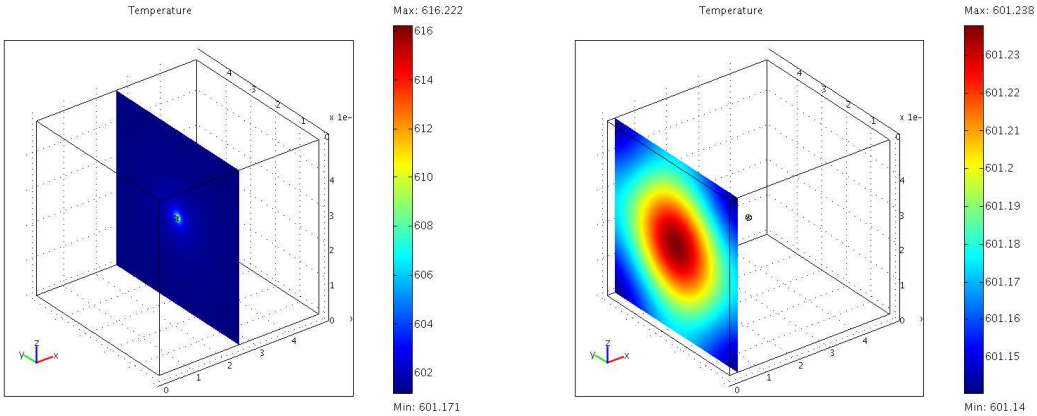

Figure 7: 3d with heating element in the middle

3 1st Order Kinetics Tube Reactor

Here we will discuss the following assumptions, assuming a uniform temperature

1. Neglecting radial effects (1d mass and species balances with an average velocity given from mass balance)
2. Neglecting axial diffusion
3. Pseudo-steady-state species balances

The motivation for the PFR assumptions, was that preliminary 2d and 3d steady-state simulations with FEMLAB (performed in May 2003) had shown a PFR type behavior; although the flow is laminar the species diffusion is sufficiently fast to assure a constant profile in radial direction, but slow enough, so that axial diffusion can be neglected. The pseudo-steady state balance are motivated from the fact that due to the small scales one can neglect the hold-up in the reactor.

For simplicity we will assume 1st order kinetics and uniform temperature with the model reaction

$$A \to 2\,B,$$

with molecular masses $M_A = 10\,\mathrm{g/mol}$ and $M_B = M_A/2$. As a reactor we are using a duct of height 0.2mm and length 5mm[5], which based on the inlet speed of 1m/s results in a nominal residence time of 5ms. We assume first order kinetics in the component A with a reaction rate, following the Arrhenius law with $k_0 = 3 \times 10^4/\mathrm{s}$ and $E_A = 2 \times 10^4 \mathrm{J/mol}$.

3.1 Scaling Analysis

3.1.1 Pseudo-steady-state mass balance

The continuity equation is:

$$\frac{\partial \rho}{\partial t} + \nabla \cdot (\rho\,\mathbf{v}) = 0. \tag{3}$$

[5]Dimensions based on the reactor designs by Arana [2, 1].

We nondimensionalize equation (3) by using the following scaling

- The time is nondimensionalized as $\tilde{t} = \frac{t}{\tau}$ so that the initial time corresponds to a value of 0 and the final time to a value of 1.
- The density is non-dimensionalized, so that for ambient temperature ($T_0 = 300\text{K}$) and pure component B, i.e., a composition $\mathbf{y}_0 = (0, 1)$, the density corresponds to 1: $\tilde{\rho}(T, \mathbf{y}) = \frac{\rho(T,\mathbf{y})}{\rho(T_0,\mathbf{y}_0)}$. The nondimensionalized density can vary from 2 (ambient temperature, pure A), to 1/3 (elevated temperature, pure B).
- The space vector is nondimensionalized by dividing through the characteristic length L: $\tilde{\mathbf{x}} = \frac{\mathbf{x}}{L}$.
- The velocity is nondimensionalized by dividing through the nominal u_{in} (at ambient temperature): $\tilde{\mathbf{v}} = \frac{\mathbf{v}}{u_{in}}$.

and we obtain

$$\frac{L}{u_{in}\,\tau}\frac{\partial\tilde{\rho}}{\partial t} + \tilde{\nabla}\cdot(\tilde{\rho}\,\tilde{\mathbf{v}}) = 0. \tag{4}$$

Since we have $L \approx 5 \times 10^{-3}\text{m}$ (taking in x direction), $\tau \approx 100\text{s}$, $u_{in} \approx 1\text{m/s}$, we obtain $\frac{L}{u_{in}\,\tau} \ll 1$ and we can assume pseudo-steady state, or neglect the hold-up in the reactor. This can be also explained by the fact that the residence time is much smaller than the time scale of change. Note also that the reference value for the density does not appear in equation (4).

Additional notes:

- If there is a drastic change in the modeling assumptions, e.g., heating time very fast, or some other fast transient, this analysis needs to be revisited
- For material constraints the short transient period might be important

3.1.2 Pseudo-steady-state species balance

Omitting the diffusion term $\nabla \mathbf{J}$, the effect of which is analyzed in section 3.1.3 and assuming 1st order Arrhenius kinetics the species balance equation reads

$$\frac{\partial C}{\partial t} + C\,\nabla \cdot \mathbf{v} + \mathbf{v} \cdot \nabla C = C\,k_0\,\exp\left(-\frac{E_A}{R\,T}\right). \tag{5}$$

Equation (5) is linear in C, so we don't need to worry about reference point and the non-dimensionalization gives[6]:

$$\frac{L}{\tau u_{in}}\frac{\partial \tilde{C}}{\partial \tilde{t}} + \tilde{C}\,\tilde{\nabla} \cdot \tilde{\mathbf{v}} + \tilde{\mathbf{v}} \cdot \tilde{\nabla}\tilde{C} = \frac{\tilde{C}\,k_0}{\tau\,u_{in}}\,\exp\left(-\frac{E_A}{R\,T}\right). \tag{6}$$

For the numerical values considered we obtain $\frac{L}{u_{in}\,\tau} \ll 1$ and we can assume pseudo-steady state. In general we cannot neglect the term $\tilde{C}\,\tilde{\nabla} \cdot \tilde{\mathbf{v}}$; also since gas expands with the production of species B, the velocity in the term $\tilde{\mathbf{v}} \cdot \tilde{\nabla}\tilde{C}$ is a function of the reactor coordinate (the residence time is lower than the nominal residence time, calculated based on inlet density).

3.1.3 1d convective flow

In our models we assume convective flow, neglecting axial diffusion and we use one-dimensional spatial distribution assuming a uniform profile in the radial direction, due to fast radial diffusion. The validity of these assumptions depends on three non-dimensional numbers

1. The ratio of height to length, here in the order of 1/100. The influence of this ratio is not trivial, but it seems that a small ratio justifies the assumptions.

2. The ratio of convection to diffusion in the axial direction (Pe=$\frac{u\,L}{D} \approx \frac{1\mathrm{m/s}\,5\times10^{-3}\mathrm{m}}{2\times10^{-5}\mathrm{m^2/s}} \approx 250$). Since this is very large, neglecting axial diffusion is a valid approximation.

3. The Damkoehler number, expressed as the ratio of reaction to diffusion $\frac{k\,d^2}{D} = \frac{d^2}{1/k\,D} \approx \frac{(50\times10^{-6}\mathrm{m})^2}{1\times10^{-3}\mathrm{s}\times2\times10^{-5}\mathrm{m^2/s}} \approx$ 0.1. So the Damkoehler number is quite small and concentration gradients in radial direction are small.

[6]Note that for different order kinetics the reaction term $\frac{\tilde{C}\,k_0}{\tau\,u_{in}}$ would contain a reference concentration.

Note that we used $d = 50\mu$m, as opposed to the tube height, because we assume the presence of catalyst support and the diffusion needs to occur between those supports.

An equivalent analysis can be performed based on the influence of four characteristic times

1. Reaction time $\frac{1}{k} \approx 1$ms.
2. Diffusion time in radial direction $\frac{d^2}{D} \approx \frac{(50\times10^{-6}\mathrm{m})^2}{2\times10^{-5}\mathrm{m}^2/\mathrm{s}} \approx 0.1$ms.
3. Diffusion time in axial direction $\frac{L^2}{D} \approx \frac{(5\times10^{-3}\mathrm{m})^2}{2\times10^{-5}\mathrm{m}^2/\mathrm{s}} \approx 1$s.
4. Residence time in reaction $\frac{L}{v} \approx 5$ms.

3.2 Simulations

For the following simulations it should be noted that we did not model surface reactions. In order to so, one would need to specify the catalyst support structure.

3.2.1 FEMLAB 2d transient simulation

We formulate a two-dimensional transient problem with a given temperature profile in time $T = 300 + 10\,t$ for a time period $t = 0 - 70$s and two modes[7]

1. Navier-Stokes equation with varying density in the continuity equation (denoted "Non-isothermal Navier Stokes" in FEMLAB)
   - The density is calculated as a function of temperature and concentration $\rho = \frac{P_{amb}}{RT}(y\,M_A + (1 - y)\,M_B)$
   - A constant viscosity of $\eta = 2.2 \times 10^{-5}$Pa s is assumed. However, since here we are not interested in pressure drops the viscosity is of little importance. The flow development is quite fast, and for developed flow the profile does not depend on the viscosity.
   - The molar fraction is calculated as a function of the temperature and concentration $\frac{C\,R\,T}{P_{amb}}$.

[7] Formulating a one-dimensional problem in FEMLAB seems to be very hard or impossible for the transient problem.

- Boundary condition at inlet: specified velocity $u = u_{in}\frac{T}{T_{amb}}$.
- Boundary condition at outlet: convective flow.
- Boundary condition at wall: no slip condition.
- Initial condition $P = P_{amb}$, $u = 0$, $v = 0$.

2. Conservative binary convection/diffusion

- A constant diffusion coefficient of $D = 2 \times 10^{-5}\mathrm{m}^2/\mathrm{s}$.
- Boundary condition at inlet: specified concentration $c = P_{amb}/(RT)$, corresponding to pure A.
- Boundary condition at outlet: convective flow.
- Boundary condition at wall: zero flux.
- Initial condition $C = P_{amb}/(RT)$, corresponding to pure A. This is not necessarily the most plausible assumption, but other initial conditions caused convergence problems. Moreover the initial conditions only affect the first ms.
- First order Arrhenius kinetics $C\,k_0\,\exp\left(-\frac{E_A}{RT}\right)$.

There are some convergence problems at the first integration step, especially when the non-conservative equation was used instead (see section 3.2.3 for an explanation of this equation), which might suggest a high index problem and which raises some doubts about the results. For the comparison in section 3.2.5 the conversion at the outlet is calculated as

$$\zeta = 1 - \frac{\frac{\int_{y=0}^{d} u(x=L,y)\,c(x=L,y)\,dy}{\int_{y=0}^{d} u(x=L,y)\,dy}}{\frac{\int_{y=0}^{d} u(x=0,y)\,c(x=0,y)\,dy}{\int_{y=0}^{d} u(x=0,y)\,dy}} \tag{7}$$

3.2.2 FEMLAB 2d steady state

In order to isolate the effect of neglecting the transient term we formulate a two dimensional quasi-steady state model, where we use the Navier-Stokes equation with varying density and the conservative convection/diffusion equation, similarly to the transient model. The comparison is performed in section 3.2.5.

The two dimensional model also allows to check the effect of using a one-dimensional model, by examining the profile in radial direction. Figure 8 shows the molfraction profile across the radial direction at various temperatures for three axial positions in the reactor, namely at 0.1, 0.5 and 1.0 of the reactor length. The profile is not constant in the cross-section, so the PFR assumption is only approximately valid.

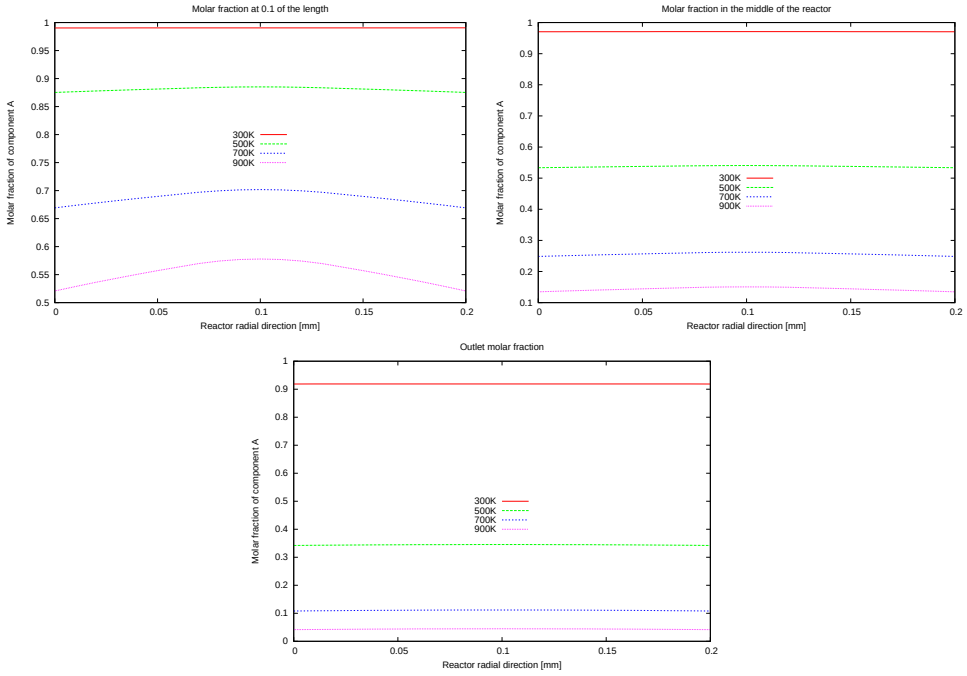

Figure 8: Concentration profile from FEMLAB

3.2.3 FEMLAB 1d steady state simulation

By assuming that diffusion in the radial direction is sufficiently fast, one can average over the radial direction. We neglect the transient term (quasi-steady-state assumption), we assume Fick diffusion and formulate a one-dimensional model in FEMLAB using the diffusion-convection equation (see also footnote 7)

$$C\,\frac{\partial u}{\partial x} + u\,\frac{\partial C}{\partial x} = C\,k_0\,\exp\left(-\frac{E_A}{R\,T(t)}\right) - D\frac{\partial C^2}{\partial x^2}, \tag{8}$$

where the velocity u can be written as a function of the concentration C. FEMLAB provides two options for the diffusion equation; in the so called non-conservative formulation the term $C\,\frac{\partial u}{\partial x}$ is omitted; in the

conservative formulation the complete equation (8) is used. Neglecting this term leads to significant mistakes because of the gas dilatation with reaction. We therefore used the conservative mode with a varying density.

3.2.4 ABACUSS 1d transient simulation

We formulated a one-dimensional spatially-discretized transient model in the process simulator ABACUSS [9, 10]. The mass and species balances are formulated as

$$\begin{aligned}
\frac{\partial u}{\partial x} &= \frac{1}{T}\frac{\partial T}{\partial t} + \frac{r}{\tilde{\rho}} \\
\frac{\partial y_A}{\partial t} &= -u\frac{\partial y_A}{\partial x} + \frac{r}{\tilde{\rho}}\,(-1 - y_A) \\
\frac{\partial y_B}{\partial t} &= -u\frac{\partial y_B}{\partial x} + \frac{r}{\tilde{\rho}}\,(2 - y_B) \\
\tilde{\rho} &= \frac{P}{RT}, \qquad (9)
\end{aligned}$$

where $\tilde{\rho}$ is the molar density and r the reaction rate. The temperature profile is given as an input variable $T = T_{amb} + 10\,t$, and its time derivative $\frac{\partial T}{\partial t}$ needs to be inserted directly, otherwise a high index problem is created. We use backward finite differences, e.g., $\frac{\partial z}{\partial x} = \frac{z_i - z_{i-1}}{\delta x}$, with a fixed stepsize δx in the axial direction. As initial conditions for the molfractions we assume $y_A(x \neq 0, t = 0) = 0$, $y_B(x, t = 0) = 1$[8] and as boundary conditions we assume $y_A(x = 0, t) = 1$ and a velocity $u = u_{in} * T/T_{amb}$.

To analyze the effects of discretization we are setting the reaction rate to zero and using mesh of different size. Figure 9 shows the molar fraction at half the reactor length as a function of time for the first milliseconds using different size mesh, with 100, 1,000 and 10,000 points. Since we do not consider diffusion, the correct profile would be a step function from 0 to 1 at time 2.5ms. As expected coarse discretization introduces numerical diffusion. To be on the safe side we therefore use 10,000 grid points for the results presented in section 3.2.5. All changes occur within ms, corresponding to the residence time, and then the influence of the initial conditions is eliminated.

[8] This initial condition corresponds to complete conversion before the startup and also allows to observe the effect of the short transient.

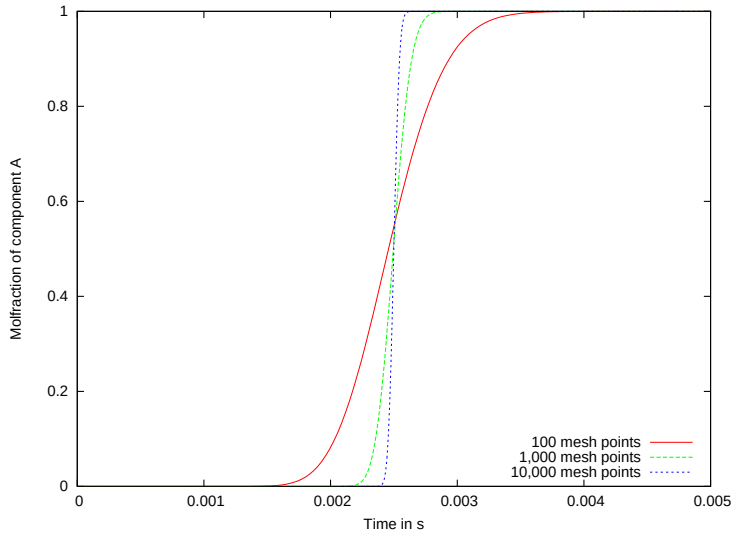

Figure 9: Transient profile of molfraction at very early times at the reactor middle for different grid sizes (without reaction).

3.2.5 Comparison of the results

In Figure 10 we compare the conversion at the outlet as a function of temperature calculated by the various models, ordered with decreasing number of ignored terms. Based on our numerical experiments we observe the following

- The effect of neglecting the transient terms is indeed very small. The comparison of transient and steady-state two dimensional models shows a very small difference while the results from transient and steady-state one dimensional models are so close to each other that one can hardly distinguish between them.

- The effect of axial diffusion is also small, as can be seen by the comparison of 1d ABACUSS and 1d Femlab model as well as by varying the diffusion coefficient in the Femlab model (not shown here).

- The effect of averaging the concentration 2d $\rightarrow$ 1d is in the order of a few % (comparison of 2d and 1d models), which is certainly acceptable[9].

[9]Even with the existence of a precise kinetic mechanism we can not be sure about the reaction rate, since the catalyst load may not be accurately known.

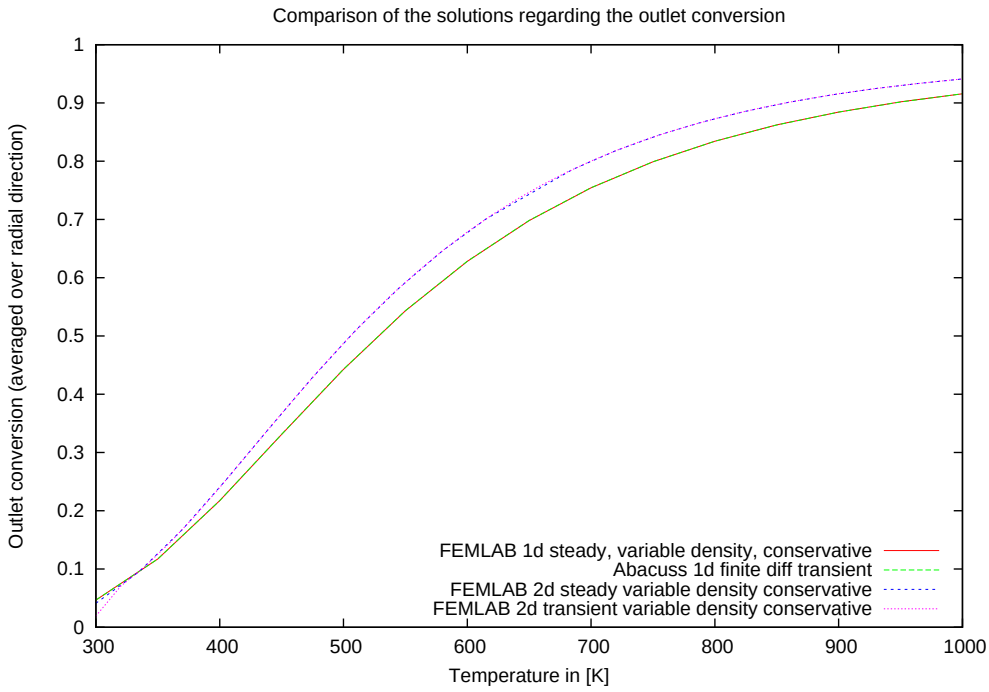

Figure 10: Comparison of conversion at the outlet as a function of the reactor temperature for the different models.

References

[1] L. R. Arana, S. B. Schaevitz, A. J. Franz, M. A. Schmidt, and K. F. Jensen. A microfabricated suspended-tube chemical reactor for thermally efficient fuel processing. *Journal of Microelectromechanical Systems*, 12(5):600–612, 2003.

[2] Leonel R. Arana. *High-Temperature Microfluidic Systems for Thermally-Efficient Fuel Processing*. PhD thesis, Massachusetts Institute of Technology, 2003.

[3] Paul I. Barton, Alexander Mitsos, and Benoît Chachuat. Optimal start-up of micro power generation processes. ESCAPE 15, May 2005.

[4] Benoît Chachuat, Alexander Mitsos, and Paul I. Barton. Optimal design and steady-state operation of micro power generation employing fuel cells. *Submitted to: Chemical Engineering Science*, Oct 2004.

[5] Benoît Chachuat, Alexander Mitsos, and Paul I. Barton. Optimal operation and design of micro power generation processes. AICHE Annual Meeting, November 2004.

[6] William M. Deen. *Analysis of Transport Phenomena*. Oxford University Press, New York, 1998.

[7] D.G. Norton and D.G. Vlachos. Combustion characteristics and flame stability at the microscale: a CFD study of premixed methane/air mixtures. *Chemical Engineering Science*, 58:4871–4882, 2003.

[8] D.G. Norton and D.G. Vlachos. A CFD study of propane/air microflame stability. *Combustion and Flame*, 138(1):97–107, 2004.

[9] John Tolsma, Jerry A. Clabaugh, and Paul I. Barton. Symbolic incorporation of external procedures into process modeling environments. *Industrial and Engineering Chemistry Research*, 41(16):3867–3876, 2002.

[10] John E. Tolsma, Jerry Clabaugh, and Paul I. Barton. http://yoric.mit.edu/abacuss2/abacuss2.html.